Multiple scattering as a diffusion process

Jos Stam

Department of Computer Science, University of Toronto
Toronto, Canada, M5S 1A4

Abstract. Multiple scattering in participating media is generally a complex phenomenon. In the limit of an optically thick medium, i.e., when the mean free path of each photon is much smaller than the medium size, the effects of multiple scattering can be approximated by a diffusion process. We introduce this approximation from the radiative transfer literature to the computer graphics community and propose several numerical methods for its solution. We implemented both a multi-grid finite differences scheme and a finite-element blob method.

1 Introduction

One of the principal aims of computer graphics is to accurately model the propagation of light. One challenge in this area is to model the propagation of light in the presence of a participating medium. Many natural environments contain participating media such as fog, steam, mist, clouds or dust. Typically in such environments each beam of light undergoes many changes as it interacts with the participating medium. The phenomenon of scattering, which changes the direction of propagation, makes this process particularly complicated. In rendering these effects, most researchers make the assumption that the light rays propagating through the medium encounter at most only one scatter event [3, 14]. To model the effects of multiple scattering, researchers either make simplifying assumptions about the participating medium or resort to expensive simulations. Rushmeier et al. assume a medium with isotropic scattering properties and derive a radiosity-style algorithm [13]. This method essentially models the interchange of energy between cubical elements (zones) of the environment. Anisotropic effects can also be modelled by discretizing the directions. These methods are known as *Discrete Ordinates* and have been applied to the rendering of participating media by Max and Languénou et al. [9, 8]. Other researchers have used direct Monte-Carlo techniques to simulate the paths of light particles in general environments [1, 11]. None of these models attempt to derive analytical models to account for the effects of multiple scattering. A notable exception is the work of Kajiya and Von Herzen [7]. They model the effects of multiple scattering by expanding the intensity field into a spherical harmonics basis. This method is known as the P_N-method in the transport theory literature, where N is the degree of the highest harmonic in the expansion [2]. Kajiya and Von Herzen derived the general method but used the P_1 expansion in their results as inferred from their statement: "We truncate the so-called "p-wave", viz. after the $l = 1$ term" [7]. In this situation, a diffusion-type equation is obtained for the scattered part of the illumination field. Unfortunately this characterization was obscured by the level of generality of their derivation. Also boundary conditions were not discussed in detail.

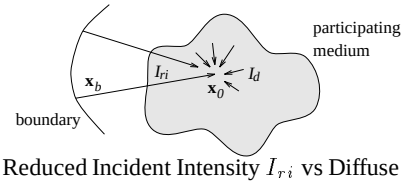

Fig. 1. Reduced Incident Intensity I_{ri} vs Diffuse Intensity I_d

The purpose of this paper is to present this *diffusion approximation* in greater detail to the computer graphics community. The approximation is valid when scattering events are frequent, i.e., in "optically thick" media. Under these exact conditions the effects of multiple scattering become apparent and the single scattering approximation is no longer valid. The effect of many scattering events is to smooth out the dependence of the intensity on its angular variable. Intuitively, in each region of the medium we find photons travelling in arbitrary directions.

The rest of the paper is organized as follows. Section 2 reviews the basic concepts and equations of transport theory. In Section 3 we show how the diffusion approximation is obtained from the transport equation. Section 4 presents numerical methods to solve diffusion equations. In Section 5 applications and results are given. Finally in Section 6 we state the conclusions and discuss future research.

2 Transport Theory

It is often convenient to separate the intensity field into two components: the *reduced incident intensity* I_{ri} and the *diffuse intensity* I_d [6]. The reduced incident intensity is that part of the intensity entering the participating medium which is attenuated by both scattering and absorption. The diffuse intensity, on the other hand, is created entirely within the medium through the phenomenon of scattering. Figure 1 illustrates the meaning of these two terms. Specifically, consider the ray $\mathbf{x}_u = \mathbf{x}_0 - u\ \mathbf{s}$ connecting a point $\mathbf{x}_b$ on one of the surfaces of the environment to a point $\mathbf{x}_0$ within the medium (again see Fig. 1). The reduced incident intensity is then the fraction of the intensity $I(\mathbf{x}_b, \mathbf{s})$ coming from the surface which is not scattered away or absorbed along the ray:

$$I_{ri}(\mathbf{x}_0, \mathbf{s}) = I(\mathbf{x}_b, \mathbf{s}) \exp\left(-\sigma_t \int_0^b \rho(\mathbf{x}_u)\ du\right),$$

where ρ is the *density* of the medium and σ_t is the *extinction cross-section* characterizing the scattering and absorptive properties of the medium. Indeed, it is the sum of a *scattering cross section* σ_s and an *absorption cross section* σ_a: $\sigma_t = \sigma_s + \sigma_a$. The *albedo* of the medium is the fraction of light that is scattered versus that which is absorbed: $\Omega = \sigma_s/\sigma_t$. Usually, there is no analytical closed form for the diffuse intensity. An equation for the diffuse intensity is obtained by equating the variation of the diffuse intensity along a given direction to the gain in intensity due to inscatter and emission minus losses caused by outscatter and absorption [6]:

$$\mathbf{s} \cdot \nabla I_d = -\sigma_t \rho (I_d + (1 - \Omega)Q + \Omega Q_{ri} + \Omega \mathcal{S}\{I_d\}), \tag{1}$$

where Q is the self-emission of the gas and $Q_{ri} = \mathcal{S}\{I_{ri}\}$ is the intensity due to the first scatter of the reduced incident intensity. The functional $\mathcal{S}$ models the effect of a single scattering event and is equal to:

$$\mathcal{S}\{I\}(\mathbf{x}, \mathbf{s}) = \frac{1}{4\pi} \int_{4\pi} p(\mathbf{s} \cdot \mathbf{s}') \; I(\mathbf{x}, \mathbf{s}') \; d\mathbf{s}', \tag{2}$$

where the *phase function* p gives the spherical distribution of light. The phase function is usually normalized such that its integral over all directions is 4π. A simple measure of the anisotropy of the participating medium is given by the *first moment* of the phase function defined by $\bar{\mu} = 3/2 \int_{-1}^{+1} \mu \; p(\mu) \; d\mu$. For negative $\bar{\mu}$ the phase function favours back scattering over forward scattering. The converse is true for positive $\bar{\mu}$. The reduced incident intensity is generally easy to calculate, since it involves only the integration of the density of the medium along a ray. A fast volume tracer can therefore be used [14, 17]. The diffuse intensity requires the solution of the transport equation and is usually more complicated to solve. In the next section we derive a diffusion equation for this intensity.

3 The Diffusion Approximation

As stated in the previous section, the diffused intensity is entirely created within the medium through the phenomenon of scattering. As the number of scattering events increases, the angular dependence tends to be smoothed out (see Appendix A). This is important since it shows that the diffuse intensity caused by many collision effects has only a weak dependence on direction. This motivates the main approximation made in the *diffusion approximation*, namely that the diffuse intensity can be expanded into the first two terms of its Taylor expansion in the directional component only:

$$I_d(\mathbf{x}, \mathbf{s}) = I_d^0(\mathbf{x}) + \mathbf{I}_d^1(\mathbf{x}) \cdot \mathbf{s}. \tag{3}$$

By substituting this reduced expansion of the diffuse intensity into Eq. 1 we obtain two equations by grouping terms that have the same order. Indeed, the left hand side of Eq. 1 becomes:

$$\mathbf{s} \cdot \nabla I_d = \mathbf{s} \cdot \nabla I_d^0 + \nabla \cdot \mathbf{I}_d^1.$$

The scattering term on the right hand side can be calculated likewise to be:[1]

$$\Omega \mathcal{S}\{I_d\} = \frac{\Omega}{4\pi} \int_{4\pi} \left(1 + \bar{\mu}(\mathbf{s} \cdot \mathbf{s}') + \cdots\right) \left(I_d^0(\mathbf{x}) + \mathbf{I}_d^1(\mathbf{x}) \cdot \mathbf{s}'\right) \; d\mathbf{s}' = \Omega I_d^0 + \frac{\Omega \bar{\mu}}{3} \mathbf{I}_d^1 \cdot \mathbf{s}.$$

Using these relations and grouping terms that have the same order, we get two equations for the coefficients I_d^0 and $\mathbf{I}_d^1$:

$$\nabla \cdot \mathbf{I}_d^1 = -\rho \left(\sigma_a I_d^0 - \sigma_s Q_{ri}^0 - \sigma_a Q\right), \tag{4}$$

$$\nabla I_d^0 = -\rho \left(\sigma_{tr} \mathbf{I}_d^1 - \sigma_s \mathbf{Q}_{ri}^1\right), \tag{5}$$

[1] We use the following identities: $\int_{4\pi} \mathbf{s}' \; d\mathbf{s}' = 0$, $\int_{4\pi} \mathbf{s} \cdot \mathbf{s}' \; d\mathbf{s}' = 0$ and $\int_{4\pi} (\mathbf{s} \cdot \mathbf{s}') \mathbf{s}' \; d\mathbf{s}' = \frac{4\pi}{3} \mathbf{s}$.

where Q^0_{ri} and $\mathbf{Q}^1_{ri}$ are the first two coefficients of Q_{ri} expanded in its angular variable. The *transport cross section* σ_{tr} is introduced as shorthand notation:

$$\sigma_{tr} = (1 - \Omega\bar{\mu}/3)\sigma_t = \sigma_s(1 - \bar{\mu}/3) + \sigma_a.$$

For constant phase functions, the flux $\mathbf{Q}^1_{ri}$ is equal to zero and the transport cross section equals the extinction cross section. These two functions, then, characterize the anisotropy of the diffuse intensity. Equations 4 and 5 are equivalent to the P_1 equations used by Kajiya and Von Herzen to render their clouds [7]. The diffusion aspect of these equations is, at this point, still hidden. We achieve a single equation for the average diffuse intensity as follows. The average flux can be extracted from the second equation and substituted into the first one to yield a diffusion equation for the average diffuse intensity:

$$\nabla \cdot \left(\kappa \nabla I^0_d\right) - \alpha I^0_d + S = 0, \tag{6}$$

where we have used the following shorthand notations:

$$\begin{aligned}
\kappa(\mathbf{x}) &= \left(\sigma_{tr}\rho(\mathbf{x})\right)^{-1}, \\
\alpha(\mathbf{x}) &= \sigma_a \rho(\mathbf{x}), \\
S(\mathbf{x}) &= \sigma_t \rho(\mathbf{x}) Q^0_{ri}(\mathbf{x}) - \frac{\sigma_s}{\sigma_{tr}} \nabla \cdot \mathbf{Q}^1_{ri}(\mathbf{x}) + \sigma_a \rho(\mathbf{x}) Q(\mathbf{x}).
\end{aligned}$$

The boundary condition that no diffuse intensity can penetrate the medium at a surface cannot be satisfied exactly, because the diffuse intensity is approximated only by its first two moments. Instead, an approximate boundary condition that the total inward flux be zero is appropriate. The exact form of this condition is [6]:

$$I^0_d(\mathbf{x}_s) - 2\kappa(\mathbf{x}_s)\frac{\partial}{\partial \mathbf{n}} I^0_d(\mathbf{x}_s) + 2\frac{\sigma_s}{\sigma_{tr}} \mathbf{n} \cdot \mathbf{Q}^1_{ri}(\mathbf{x}_s) = 0, \tag{7}$$

for all points $\mathbf{x}_s$ lying on the boundary and $\mathbf{n}$ denotes the normal to the surface at point $\mathbf{x}_s$. Once the average diffuse intensity has been calculated, we can compute the average flux from Equation 5:

$$\mathbf{I}^1_d(\mathbf{x}) = \kappa(\mathbf{x}) \left(-\nabla I^0_d(\mathbf{x}) + \sigma_s \rho(\mathbf{x}) \mathbf{Q}^1_{ri}(\mathbf{x})\right). \tag{8}$$

In other words, the diffuse intensity is determined essentially by its first coefficient, since the flux $\mathbf{I}^1_d$ is proportional to the gradient of I^0_d.

The diffusion equation can also be obtained by expanding the intensity field into a perturbation series in the dimensionless ratio l/L_0, where $l = 1/\sigma_t\rho$ is the *mean free path* of the photons and L_0 is a characteristic length of the medium, e.g., $L_0 = 100$ km for clouds and $L_0 = 1$ m for steam rising from a kettle. When this ratio is small, local interactions dominate and the global transport equation collapses into a diffusion equation. The approximation is commonly considered valid when this ratio is smaller than $1/4$ [15].

From this diffusion equation, we can now make certain qualitative remarks concerning the phenomenon of multiple scattering. The basic effect is to smear out the initial source intensity S equal to the first scatter and the self-emission of the gas over time.

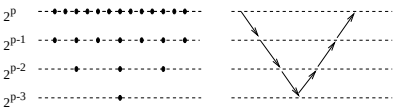

Fig. 2. The multi-grid method and a "v"-cycle

The effects of multiple scattering are most pronounced when the diffusion coefficient is high and the absorption rate is low. Specifically, the diffusion constant is higher for phase functions favouring forward scattering ($\bar{\mu} > 0$) versus backward scattering. The same is achieved when the albedo is close to unity. Chiefly, clouds have both a high albedo and a strong forward scattering. Multiple scattering is therefore an important phenomenon in clouds.

In the next section we will review some numerical techniques to solve the diffusion equation.

4 Numerical Solution of the Diffusion Equation

4.1 Multi-Grid Schemes

We obtain a straightforward numerical scheme for the diffusion equation when both the diffuse intensity and the source intensity are discretized on a three-dimensional grid of size N^3 and spacing h. The diffusion operator is then approximated using central differences:

$$\nabla\kappa\nabla I \approx \frac{\kappa_{i+1,j,k}I_{i+1,j,k} + \kappa_{i-1,j,k}I_{i-1,j,k} + \cdots + \kappa_{i,j,k-1}I_{i,j,k-1} - 6I_{i,j,k}}{h^2},$$

where $\kappa_{i,j,k}$ is the sampled version of the diffusion constant. This discretization yields a system of equations for the interior points of the domain. For large N this system cannot be solved directly and is usually solved by relaxation [12]. After each relaxation step, we update the boundary by discretizing Equation 7. Let (i, j, k) be a point on the boundary. The variation along the normal is then approximated by:

$$\frac{\partial}{\partial \mathbf{n}} I_{i,j,k} \approx \frac{I_{i',j',k'} - I_{i,j,k}}{h},$$

where (i', j', k') is the closest sample to the boundary along the normal. For example, for the boundary point $(i, 0, k)$, the closest point is $(i, 1, k)$. The boundary condition is thus satisfied if the boundary is updated after each relaxation step:

$$I_{i,j,k} = \frac{2\kappa_{i,j,k}I_{i',j',k'} - 2h\ \mathbf{n}\cdot\mathbf{Q}_{i,j,k}}{h + 2\kappa_{i,j,k}},$$

where $\mathbf{Q}_{i,j,k}$ is the sampled version of the function $\sigma_s/\sigma_{tr}\mathbf{Q}^1_{ri}$.

A major drawback of relaxation schemes is their slow convergence. A powerful technique to speed up the convergence rate is to relax the system on grids with different spacings h. Following we will briefly review this method, known as the *multi-grid method* (for more details see [4]). The efficiency of the multi-grid method is due to both

the fact that it can produce a good initial estimate of the solution and that it removes the high frequencies from the error by relaxing on coarser grids. These are achieved by considering a hierarchy of grids of spacings $h = 2^p$, $p = p_{coarse}, \ldots, p_{fine}$. The equation is first relaxed on the finest grid for a fixed number of iterations and then projected onto the next coarsest grid. This projection is likewise relaxed for a fixed number of iterations. These two steps are repeated until the coarsest level has been reached. The whole process is then reversed: each approximation is interpolated and relaxed on to the next finer grid. This process is repeated until the finest grid is reached. The above procedure corresponds to a complete "v-cycle" as illustrated in Figure 2. An approximation of the solution is attained by going through a fixed number of such v-cycles until convergence. In practice, the multi-grid is an order of magnitude faster then straightforward relaxation. However, this method is very memory intensive for large three-dimensional domains. Therefore, we propose an alternative method of solution corresponding to a finite element scheme.

4.2 Blob Finite Element Method

We obtain an alternate finite representation of the diffuse intensity by expanding it into a set of basis functions. We have chosen to experiment with a "blob representation" of the intensity field [18]:

$$I_d^0(\mathbf{x}) = 1/\rho(\mathbf{x}) \sum_{i=1}^{N} I_i m_i G(\mathbf{x} - \mathbf{x}_i, \sigma_i),$$

where m_i, $\mathbf{x}_i$ and σ_i model the mass, center and size of the blob, respectively. The *smoothing kernel* depends usually on distance alone and is taken here to be a Gaussian "bell" function. By inserting this representation into Eq. 6 and setting $\mathbf{x} = \mathbf{x}_j$ ($j = 1, \cdots, N$) we obtain a set of N equations:

$$\sum_{i=1}^{N} m_i I_i (\nabla \kappa(\mathbf{x}_j) \nabla G_{ij} - \alpha(\mathbf{x}_j) G_{ij}) + S(\mathbf{x}_j) = 0,$$

where $G_{ij} = G(\mathbf{x}_j - \mathbf{x}_i, \sigma_i)/\rho(\mathbf{x}_j)$. This method is actually a *collocation method* [10]. Care should be taken that the centers of the blobs are not too proximate, to avoid numerical instabilities. The system can be solved by LU decomposition when the number of blobs is below 200 or so [12].

5 Applications and Results

5.1 Light Beam in a Constant Density Atmosphere

In the first application we show the effects of the various parameters of the diffusion equation for a simple case of a constant density ρ_0 illuminated by a beam of light. For simplicity, the propagation is limited to a two-dimensional domain. We assume that the initial intensity S_0 of the beam is concentrated on the lower part of the plane

corresponding to the x-axis. Then the source term of the diffusion equation can be computed analytically [6]:

$$S(x,y) = \rho_0 \left(\sigma_s + \sigma_s \sigma_t / \sigma_{tr} \overline{\mu}\right) S_0(x) \exp(-\rho_0 \sigma_t y).$$

The flux $\mathbf{Q}_{i,j}$ appearing in the boundary conditions can be computed likewise to be:

$$\mathbf{Q}_{i,j} = \frac{\sigma_s \overline{\mu}}{\sigma_{tr}} S^0(hi) \exp(-\sigma_t \rho_0 hj)(0,1).$$

We have implemented the multi-grid finite difference scheme on a grid of size 512×512 with a "v"-cycle of depth 5. Only three relaxation steps were performed on each level. The solution of the diffusion equation took approximately 30 seconds on an SGI Indigo with an RS4000 processor. The following pictures depict both the diffuse intensity and the sources. Figure 3 shows the effects of the following parameters on the diffusion process: albedo Ω, extinction cross-section σ_t and the first moment of the phase function $\overline{\mu}$. As predicted, the diffusion is strongest for forward scattering in high albedo media.

5.2 Non-Constant Densities

Now we apply the diffusion approximation to a participating medium with a non-constant density distribution lit by a directional light source from above. We assume that the density is modelled as a superposition of the N Gaussian blobs [18]. In this case, the diffuse intensity drops off to zero at the edge of the density and the boundary conditions are satisfied naturally by the blob finite elements [10]. As in the previous example we used a two-dimensional domain. Each picture was rendered by assuming that the domain has a certain thickness l. The final intensity for each pixel (x,y) is then calculated by:

$$I(x,y) = \tau(x,y) I_{back} + (1 - \tau(x,y)) I_{i,j} \qquad \text{where} \quad \tau(x,y) = \exp\left(-\sigma_t \rho(x,y) l\right),$$

where $x = ih$ and $y = hj$. In our pictures we have set $l = 100$ and the background colour I_{back} to blue. We have computed solutions for two different numbers of blobs. The results are shown in Figure 5 and are compared to a multi-grid finite difference solution. The top pictures display the source term for each method. The source term is sampled at the center of each blob in the finite element method. The pictures at the bottom show the result after diffusion. The results demonstrate that the diffusion approximation does a fairly good job at approximating the solution given by the multi-grid scheme. This is achieved by using a discretization, which is an order of magnitude more efficient both in terms of storage (76 versus $512^2 = 262144$ elements) and computation time (0.2 versus 30 seconds). The blob solution could be used in an interactive graphics package.

5.3 Other Applications

Another potential application is the calculation of diffuse light from surfaces due to subsurface scattering. Hanrahan and Krueger calculated the effect of multiple scattering in the sub-surface layer using a Monte-Carlo simulation technique [5]. The multi-grid diffusion scheme could be used on a thin slice corresponding to one of the subsurface

layers. The source intensity driving the diffusion process is equal to the refracted light incident on the surface. However, because boundary conditions are only approximate in the diffusion approximation, the results of such a simulation might not be sufficiently accurate.

6 Conclusions and Future Research

In this paper we have presented and explored applications of the diffusion approximation from transport theory to computer graphics. We have introduced a multi-grid solution to this equation that is efficient for nearly two-dimensional (thin slice) domains. In three-dimensions, this method suffers from the problems associated with grid-based methods: high computation costs and high storage requirements. To alleviate this problem, we have proposed an efficient finite element method based on Gaussian blobs to calculate the effects of multiple scattering in media with non-constant densities. The blob method gives a fairly good approximation, using far less memory and computation time. The accuracy of the diffusion approximation itself has not been tested rigorously. We intend to compare our results with the solutions obtained via Discrete Ordinates [8].

Acknowledgements

Thanks to Eugene Fiume for supervising this work, to Eric Languénou for many stimulating discussions and to Pamela Jackson for proofreading the paper.

A Proof of Angular Smoothing Due to Multiple Scattering

Both the phase function and the angular component of the intensity field can be expanded into spherical harmonics [16, 2]:

$$\begin{aligned} p(\mathbf{s}\cdot\mathbf{s}') &= \sum_{l=0}^{\infty}\sum_{m=-l}^{l} p_l Y^*_{l,m}(\mathbf{s}')Y_{l,m}(\mathbf{s}), \\ I(\mathbf{x},\mathbf{s}) &= \sum_{l'=0}^{\infty}\sum_{m'=-l'}^{l'} I_{l',m'}(\mathbf{x})Y_{l',m'}(\mathbf{s}), \end{aligned}$$

in particular $p_0 = 4\pi$ and $p_1 = 2\pi\bar{\mu}/3$. We are not concerned with the exact form of the harmonics. However, we do use the property that they form an orthonormal basis of the functions defined on the unit sphere:

$$\int_{4\pi} Y^*_{l',m'}(\mathbf{s})Y_{l,m}(\mathbf{s})\; d\mathbf{s} = \delta_{l',l}\delta_{m',m}\,.$$

Consequently, a single scatter event becomes a simple multiplication by the coefficients of the phase function:

$$\mathcal{S}\{I\}(\mathbf{x},\mathbf{s}) = \sum_{l',m'}\sum_{l,m} p_l I_{l',m'}(\mathbf{x})Y_{l,m}(\mathbf{s})\frac{1}{4\pi}\int_{4\pi} Y^*_{l,m}(\mathbf{s}')Y_{l',m'}(\mathbf{s}')\; d\mathbf{s}'$$

$$= \sum_{l,m} \frac{p_l}{4\pi} I_{l,m}(\mathbf{x}) Y_{l,m}(\mathbf{s}).$$

The accumulative effect on the intensity field of n scattering events at a location $\mathbf{x}$ can be expressed through the scattering functional $\mathcal{S}$ (see Eq. 2) as

$$\mathcal{S}^n\{I\}(\mathbf{x},\mathbf{s}) = \mathcal{S}^{n-1}\{\mathcal{S}\{I\}\}(\mathbf{x},\mathbf{s}) = \sum_{l=0}^{\infty} \sum_{m=-l}^{l} \left(\frac{p_l}{4\pi}\right)^n I_{l,m}(\mathbf{x}) Y_{l,m}(\mathbf{s}).$$

This last expression tends towards $I_{0,0}(\mathbf{x})$ as n tends towards infinity. This is a consequence of the fact that each coefficient p_l is strictly smaller than 4π in absolute value, with the exception of the first one. This demonstrates that the dependence of the intensity field diminishes as the number of scatter events n increases.

References

1. P. Blasi, B. Le Saec, and C. Schlick. "A Rendering Algorithm for Discrete Volume Density Objects". *Computer Graphics Forum*, 12(3):201–210, 1993.
2. J. J. Duderstadt and W. R. Martin. *Transport Theory*. John Wiley and Sons, New York, 1979.
3. D. S. Ebert and R. E. Parent. "Rendering and Animation of Gaseous Phenomena by Combining Fast Volume and Scanline A-buffer Techniques". *ACM Computer Graphics (SIGGRAPH '90)*, 24(4):357–366, August 1990.
4. W. Hackbusch. *Multi-grid Methods and Applications*. Springer Verlag, Berlin, 1985.
5. P. Hanrahan and W. Krueger. "Reflection from Layered Surfaces due to Subsurface Scattering". In *Proceedings of SIGGRAPH '93*, pages 165–174. Addison-Wesley Publishing Company, August 1993.
6. A. Ishimaru. *VOLUME 1. Wave Propagation and Scattering in Random Media. Single Scattering and Transport Theory*. Academic Press, New York, 1978.
7. J. T. Kajiya and B. P. von Herzen. "Ray Tracing Volume Densities". *ACM Computer Graphics (SIGGRAPH '84)*, 18(3):165–174, July 1984.
8. E. Languénou, K.Bouatouch, and M.Chelle. Global illumination in presence of participating media with general properties. In *Proceedings of the 5th Eurographics Workshop on Rendering*, pages 69–85, Darmstadt, Germany, June 1994.
9. N. Max. Efficient light propagation for multiple anisotropic volume scattering. In *Proceedings of the 5th Eurographics Workshop on Rendering*, pages 87–104, Darmstadt, Germany, June 1994.
10. D. H. Norrie and G. de Vries. *The Finite Element Method. Fundamentals and Applications*. Academic Press, New York, 1973.
11. S. N. Pattanaik and S. P. Mudur. Computation of global illumination in a participating medium by monte carlo simulation. *The Journal of Visualization and Computer Animation*, 4(3):133–152, July–September 1993.

12. W. H. Press, B. P. Flannery, S. A. Teukolsky, and W. T. Vetterling. *Numerical Recipes in C. The Art of Scientific Computing*. Cambridge University Press, Cambridge, 1988.

13. H. E. Rushmeier and K. E. Torrance. "The Zonal Method for Calculating Light Intensities in the Presence of a Participating Medium". *ACM Computer Graphics (SIGGRAPH '87)*, 21(4):293–302, July 1987.

14. G. Sakas. "Fast Rendering of Arbitrary Distributed Volume Densities". In F. H. Post and W. Barth, editors, *Proceedings of EUROGRAPHICS '90*, pages 519–530. Elsevier Science Publishers B.V. (North-Holland), September 1990.

15. R. Siegel and J. R. Howell. *Thermal Radiation Heat Transfer*. Hemisphere Publishing Corp., Washington DC, 1981.

16. F. X. Sillion, J. R. Arvo, S. H. Westin, and D. P. Greenberg. "A Global Illumination Solution for General Reflectance Distributions". *ACM Computer Graphics (SIGGRAPH '91)*, 25(4):187–196, July 1991.

17. J. Stam and E. Fiume. "Turbulent Wind Fields for Gaseous Phenomena". In *Proceedings of SIGGRAPH '93*, pages 369–376. Addison-Wesley Publishing Company, August 1993.

18. J. Stam and E. Fiume. "Depicting Fire and Other Gaseous Phenomena Using Diffusion Processes". To appear in SIGGRAPH'95, 1995.

Fig. 3. Effect of Varying Ω, σ_t and $\bar{\mu}$

Fig. 4. Non-Constant Densities